

Ground-based Remote-sensing Synergy for Cloud Properties and Aerosol-Cloud Interactions

Authors: Jana Preißler, Giovanni Martucci and Colin D. O'Dowd



ENVIRONMENTAL PROTECTION AGENCY

The Environmental Protection Agency (EPA) is responsible for protecting and improving the environment as a valuable asset for the people of Ireland. We are committed to protecting people and the environment from the harmful effects of radiation and pollution.

The work of the EPA can be divided into three main areas:

Regulation: *We implement effective regulation and environmental compliance systems to deliver good environmental outcomes and target those who don't comply.*

Knowledge: *We provide high quality, targeted and timely environmental data, information and assessment to inform decision making at all levels.*

Advocacy: *We work with others to advocate for a clean, productive and well protected environment and for sustainable environmental behaviour.*

Our Responsibilities

Licensing

We regulate the following activities so that they do not endanger human health or harm the environment:

- waste facilities (*e.g. landfills, incinerators, waste transfer stations*);
- large scale industrial activities (*e.g. pharmaceutical, cement manufacturing, power plants*);
- intensive agriculture (*e.g. pigs, poultry*);
- the contained use and controlled release of Genetically Modified Organisms (*GMOs*);
- sources of ionising radiation (*e.g. x-ray and radiotherapy equipment, industrial sources*);
- large petrol storage facilities;
- waste water discharges;
- dumping at sea activities.

National Environmental Enforcement

- Conducting an annual programme of audits and inspections of EPA licensed facilities.
- Overseeing local authorities' environmental protection responsibilities.
- Supervising the supply of drinking water by public water suppliers.
- Working with local authorities and other agencies to tackle environmental crime by co-ordinating a national enforcement network, targeting offenders and overseeing remediation.
- Enforcing Regulations such as Waste Electrical and Electronic Equipment (WEEE), Restriction of Hazardous Substances (RoHS) and substances that deplete the ozone layer.
- Prosecuting those who flout environmental law and damage the environment.

Water Management

- Monitoring and reporting on the quality of rivers, lakes, transitional and coastal waters of Ireland and groundwaters; measuring water levels and river flows.
- National coordination and oversight of the Water Framework Directive.
- Monitoring and reporting on Bathing Water Quality.

Monitoring, Analysing and Reporting on the Environment

- Monitoring air quality and implementing the EU Clean Air for Europe (CAFÉ) Directive.
- Independent reporting to inform decision making by national and local government (*e.g. periodic reporting on the State of Ireland's Environment and Indicator Reports*).

Regulating Ireland's Greenhouse Gas Emissions

- Preparing Ireland's greenhouse gas inventories and projections.
- Implementing the Emissions Trading Directive, for over 100 of the largest producers of carbon dioxide in Ireland.

Environmental Research and Development

- Funding environmental research to identify pressures, inform policy and provide solutions in the areas of climate, water and sustainability.

Strategic Environmental Assessment

- Assessing the impact of proposed plans and programmes on the Irish environment (*e.g. major development plans*).

Radiological Protection

- Monitoring radiation levels, assessing exposure of people in Ireland to ionising radiation.
- Assisting in developing national plans for emergencies arising from nuclear accidents.
- Monitoring developments abroad relating to nuclear installations and radiological safety.
- Providing, or overseeing the provision of, specialist radiation protection services.

Guidance, Accessible Information and Education

- Providing advice and guidance to industry and the public on environmental and radiological protection topics.
- Providing timely and easily accessible environmental information to encourage public participation in environmental decision-making (*e.g. My Local Environment, Radon Maps*).
- Advising Government on matters relating to radiological safety and emergency response.
- Developing a National Hazardous Waste Management Plan to prevent and manage hazardous waste.

Awareness Raising and Behavioural Change

- Generating greater environmental awareness and influencing positive behavioural change by supporting businesses, communities and householders to become more resource efficient.
- Promoting radon testing in homes and workplaces and encouraging remediation where necessary.

Management and structure of the EPA

The EPA is managed by a full time Board, consisting of a Director General and five Directors. The work is carried out across five Offices:

- Office of Environmental Sustainability
- Office of Environmental Enforcement
- Office of Evidence and Assessment
- Office of Radiation Protection and Environmental Monitoring
- Office of Communications and Corporate Services

The EPA is assisted by an Advisory Committee of twelve members who meet regularly to discuss issues of concern and provide advice to the Board.

EPA RESEARCH PROGRAMME 2014–2020

Ground-based Remote-sensing Synergy for Cloud Properties and Aerosol–Cloud Interactions

(2012-CCRP-FS.13)

EPA Research Report

Prepared for the Environmental Protection Agency

by

National University of Ireland, Galway

Authors:

Jana Preißler, Giovanni Martucci and Colin D. O'Dowd

ENVIRONMENTAL PROTECTION AGENCY

An Ghníomhaireacht um Chaomhnú Comhshaoil
PO Box 3000, Johnstown Castle, Co. Wexford, Ireland

Telephone: +353 53 916 0600 Fax: +353 53 916 0699
Email: info@epa.ie Website: www.epa.ie

ACKNOWLEDGEMENTS

This report is published as part of the EPA Research Programme 2014–2020. The EPA Research Programme is a Government of Ireland initiative funded by the Department of Communications, Climate Action and Environment. It is administered by the Environmental Protection Agency, which has the statutory function of co-ordinating and promoting environmental research.

DISCLAIMER

Although every effort has been made to ensure the accuracy of the material contained in this publication, complete accuracy cannot be guaranteed. The Environmental Protection Agency, the authors and the steering committee members do not accept any responsibility whatsoever for loss or damage occasioned, or claimed to have been occasioned, in part or in full, as a consequence of any person acting, or refraining from acting, as a result of a matter contained in this publication. All or part of this publication may be reproduced without further permission, provided the source is acknowledged.

The EPA Research Programme addresses the need for research in Ireland to inform policymakers and other stakeholders on a range of questions in relation to environmental protection. These reports are intended as contributions to the necessary debate on the protection of the environment.

EPA RESEARCH PROGRAMME 2014–2020

Published by the Environmental Protection Agency, Ireland

ISBN: 978-1-84095-809-6

January 2019

Price: Free

Project Partners

Dr Jana Preißler

School of Physics
Centre for Climate and Air Pollution Studies
Ryan Institute
National University of Ireland Galway
Galway
Ireland
Tel.: +353 91 495 468
Fax: +353 91 494 584
Email: jana.preissler@nuigalway.ie

Professor Colin O'Dowd

School of Physics
Centre for Climate and Air Pollution Studies
Ryan Institute
National University of Ireland Galway
Galway
Ireland
Tel.: +353 91 493 306
Fax: +353 91 494 584
Email: colin.odowd@nuigalway.ie

Dr Giovanni Martucci

Federal Office of Meteorology and Climatology
MeteoSwiss
Ch. De l'Aérologie
CH-1530 Payerne
Switzerland
Email: giovanni.martucci@meteoswiss.ch

Contents

Acknowledgements	ii
Disclaimer	ii
Project Partners	iii
List of Figures	vi
Executive Summary	vii
1 Introduction	1
2 The Influence of Aerosols on Cloud Microphysics and Radiative Forcing	3
2.1 Instruments and Methods	3
2.2 The Data Set	4
2.3 Microphysical Cloud Properties	4
2.4 Optical Cloud Properties	5
2.5 Summary	6
3 The Impact of Hemispheric Transboundary Air Pollution on Cloud Microphysics	7
3.1 Aerosol Detection	7
3.2 Aerosol Quantification	8
3.3 Summary	10
4 The Sensitivity of the Cloud Microphysical System to Both Natural and Anthropogenic Aerosols	11
5 WP 1: Retrieval of the Aerosol Optical Parameters	12
6 WP 2: Quantification of the Aerosol Indirect Effect	13
7 Summary and Conclusions	18
8 Recommendations	19
References	20
Abbreviations	22

List of Figures

Figure 2.1.	Distributions of CDNC (top, on logarithmic scale), effective radius (r_{eff} , centre) and LWC (bottom) by air mass transport	4
Figure 2.2.	Distributions of COT (top) and cloud albedo (bottom) by air mass transport. Modified air masses (mar. mod., marine modified; cont. mod., continental modified) are plotted as lines	5
Figure 3.1.	Aerosol detection product of observations from Mace Head on 20 May 2015	7
Figure 3.2.	Aerosol detection product of observations from Mace Head on 19 April 2010	8
Figure 3.3.	Logarithm of the extinction coefficient (in km^{-1}) from ceilometer observations on 20 May 2015	9
Figure 3.4.	Aerosol mass concentration (in g m^{-2}) from ceilometer observations on 20 May 2015	9
Figure 6.1.	Box plots of the concentrations of (a) BC, (b) CCN, (c) SO_4 and (d) sea salt (SS), sorted by the air mass transport according to back-trajectories (mar. mod., marine modified; cont. mod., continental modified)	13
Figure 6.2.	Distributions of (a) the effective radius, (b) CDNC, (c) LWC and (d) COD by condensation nuclei (CN) concentration	14
Figure 6.3.	Distributions of (a) the effective radius, (b) CDNC, (c) LWC and (d) COD by BC concentration	15
Figure 6.4.	Distributions of (a) the effective radius, (b) CDNC, (c) LWC and (d) COD by SO_4 concentration	15
Figure 6.5.	Aerosol indirect effect normalised by cloud depth using different cloud proxies (symbols) vs. the BC concentration, colour coded by air mass transport path. R_{eff} , effective radius	16

Executive Summary

A synergistic combination of long-term remote sensing and *in situ* observations was used to investigate the impact of both natural marine and anthropogenic aerosols on clouds and cloud optical properties. Homogeneous single-layer non-precipitating water clouds were carefully selected from a database spanning more than 6 years. This comprehensive study of 118 cloud cases with a total of more than 18,000 data points (time steps) can be considered as statistically representative. The results confirm the theory and previous findings of an increase in cloud droplet number concentration (CDNC) and decrease in cloud droplet effective radius with increasing pollution. The cloud optical thickness (COT) and albedo were lower in cleaner air masses and higher in more polluted conditions.

The quantification of aerosols in terms of particle extinction coefficient and mass concentration could not be realised as originally proposed because of problems with the newly purchased Raman lidar. Ceilometer data were used instead to quantify aerosols within limitations and under large uncertainties.

Instead of the initially proposed Raman lidar data, *in situ* data from an aerosol mass spectrometer, a scanning mobility particle sizer, an aerodynamic particle sizer, an aerosol chemical speciation monitor and a tapered element oscillating microbalance were used in an attempt to quantify the aerosol indirect effect on microphysical cloud properties. In order to verify the representativeness of the aerosol concentration levels near the surface for the aerosol concentrations at cloud altitudes, these observations were combined with back-trajectories.

Improvement in aerosol quantification using ground-based remote sensing at Mace Head is strongly recommended for a better understanding of the impact of aerosols on cloud properties in the future. Continued work on the SYSOC (SYnergistic Remote Sensing Of Clouds) algorithm to reduce the uncertainties is also recommended.

1 Introduction

The overall objective of the GAINFUL (Ground-bAsed remote-sensING and in-situ aerosol-cloud synergy For hemispheric trans-boUndary air poLLution studies) project was to reduce the uncertainty of the impact of both natural marine and anthropogenic aerosols on clouds and cloud optical properties using long-term observations and synergetic *in situ* and remote-sensing techniques. The project was based on the combination of continuous ground-based *in situ* observations of aerosols, including aerosol mass spectrometric techniques, with synergistic ground-based remote-sensing retrievals of aerosol optical parameters and liquid cloud microphysics at the Mace Head World Meteorological Organization/ Global Atmosphere Watch (WMO/GAW) station. The aim was to retrieve microphysical properties of liquid water clouds using two state-of-the-art techniques. A database of optical aerosol parameters and cloud microphysical products was also planned, with the ultimate goal of advancing our understanding of key processes associated with aerosol–cloud interactions.

Aerosols and clouds both cause direct radiative forcing by scattering and absorbing solar and infrared radiation in the atmosphere. In the last century, with the global increase in their average load, aerosols have most likely made a significant negative contribution to the overall radiative forcing. In fact, the Intergovernmental Panel on Climate Change (IPCC) fourth assessment report (AR4; Solomon *et al.*, 2007) indicates a $-0.5 \pm 0.4 \text{ W m}^{-2}$ cooling effect as a result of the anthropogenic component of the total aerosol in the atmosphere. Through their role as nuclei of condensation, aerosols also alter liquid water, ice and mixed-phase cloud formation processes by increasing droplet number concentrations and ice particle concentrations. They can suppress precipitation from warm clouds and thereby cause an indirect radiative forcing associated with these changes in cloud properties. However, the determination of the global cloud radiative forcing and the impact of aerosols on it is affected by large uncertainties, especially concerning the lifetime effect (prolonged cloud lifetime due to suppressed precipitation) and the droplet size distribution (AR5; Stocker *et al.*, 2013).

The ground-based remote-sensing suite at Mace Head includes a cloud radar, a ceilometer, a microwave radiometer and a Doppler wind lidar. Those instruments are complemented by a large number of ground-based *in situ* instruments, including an aerosol mass spectrometer (AMS), a scanning mobility particle sizer (SMPS), an aerodynamic particle sizer (APS), an aerosol chemical speciation monitor (ACSM) and a tapered element oscillating microbalance (TEOM).

This project had three main goals:

- to study the influence of natural and anthropogenic aerosols on cloud microphysics and radiative forcing;
- to quantify the impact of hemispheric transboundary air pollution on cloud microphysics;
- to quantify the sensitivity of the cloud microphysical system to both natural and anthropogenic aerosols.

Those goals were originally addressed in the following two work packages and corresponding tasks:

1. Retrieval and creation of a database of the aerosol optical parameters such as backscatter, extinction and mass extinction:
 - acquisition of the new R-MAN 510 Raman lidar at Mace Head and generation of quality-assured aerosol optical parameters, e.g. backscatter (β) and extinction (σ);
 - creation of a $[\beta - \sigma]$ -database;
 - evaluation of lidar-derived mass extinction coefficients for clean air aerosols;
 - evaluation of lidar-derived mass extinction coefficients for polluted air aerosols.
2. Quantification of the aerosol indirect effect (AIE) from synergistic *in situ* and ground-based remote-sensing cloud microphysics:
 - evaluation of the particulate matter ($\text{PM}_{1-2.5}$ and PM_{10}) impact on cloud microphysics;
 - evaluation of ACSM continuous physical–chemical speciation of clean and polluted aerosol impacts on cloud microphysics;

- evaluation of the SMPS-weighted size distribution and high-resolution time of flight (HR-TOF) AMS-derived aerosol mass concentration impact on cloud microphysics;
 - calibration of the aerosol and cloud microphysical products obtained using different retrieval methods against the common *in situ* ACSM and HR-TOF AMS references at Mace Head;
 - sensitivity analysis of the AIE with regard to new proxies in order to reduce the uncertainty affecting the quantification of the AIE;
 - creation of a database of quality-assured AIE values.
- The three main objectives and two work packages are addressed in the following chapters.

2 The Influence of Aerosols on Cloud Microphysics and Radiative Forcing

One objective of this fellowship was to study the influence of natural and anthropogenic aerosols on cloud microphysics and radiative forcing. The microphysical and optical cloud properties were obtained using a synergistic combination of cloud radar, ceilometer and microwave radiometer data. This work was recently submitted in more detail to the *Journal of Geophysical Research: Atmospheres* (Preißler *et al.*, 2016).

2.1 Instruments and Methods

The radar used was a MIRA36, 35.5-GHz Ka-band Doppler cloud radar (Bauer-Pfundstein and Goersdorf, 2007; Melchionna *et al.*, 2008) that measures the reflectivity, the linear depolarisation ratio and the vertical velocity. The ceilometer used was a CHM15K from Jenoptik (Heese *et al.*, 2010; Martucci *et al.*, 2010) measuring at 1064 nm. It detects photons backscattered from atmospheric targets such as cloud droplets or aerosol particles. It is capable of detecting aerosol layers as well as clouds up to a certain penetration depth, depending on the cloud optical depth (COD). The microwave radiometer used was an RPG-HATPRO (Crewell and Löhnert, 2003; Löhnert and Crewell, 2003; Löhnert *et al.*, 2009) water vapour and oxygen multi-channel microwave profiler (Martucci and O'Dowd, 2011) that delivers profiles of the temperature and humidity. This set of instruments enables the vertically resolved determination of microphysical cloud properties such as cloud droplet number concentration (CDNC), cloud droplet effective radius and liquid water content (LWC) from the ground. The algorithm SYRSOC (SYnergistic Remote Sensing Of Clouds) was used to retrieve these microphysical cloud properties as well as the optical properties of COD and cloud albedo. SYRSOC works under the assumptions of a mono-modal droplet size distribution and uses an explicit subadiabaticity scheme to describe the adiabatic departure of the LWC profile at each altitude. It has been described in detail by Martucci and O'Dowd (2011).

In the framework of this fellowship, the SYRSOC software package has been automated and is now independent of human interference. It is instead linked to a MySQL database containing all required input parameters, as well as mean results. In addition, a manual for the complex set of algorithms was written with the objective of facilitating the sharing of SYRSOC and thus encouraging international collaborations.

A systematic overestimation of the CDNC calculated from the ceilometer extinction was detected by comparison of the SYRSOC results with ground-based cloud condensation nuclei (CCN) measurements. This issue has been investigated in detail and it was found that the calibration approach for the ceilometer backscatter coefficient, and consequently the extinction coefficient, is not valid for all cloud cases. A so-called Rayleigh calibration (normalisation of the ceilometer attenuated backscatter with the molecular backscatter) was performed during clear nights and thus a calibration constant was obtained. However, this constant is not valid for daytime measurements, as the instrument changes its sensitivity in order to protect the sensitive detectors from overload due to high background radiation. The sensitivity is even further reduced in case of very low optically thick clouds because of the sudden peak in the received backscattered radiation. A daytime calibration of the ceilometer is possible by combination with sun photometer data. The integrated extinction profile of the ceilometer is matched to the aerosol optical depth determined by the sun photometer. The obtained calibration constant could thus be used for daytime measurements. As the sensitivity, and hence the calibration constant, change in case of certain cloud types, another approach must be found to correct for these changes. As this abrupt change is evident through the whole profile (sudden drop in signal from one time step to the next), this problem could be corrected by using a height constant factor. For this work, however, the CDNC was calculated using the cloud radar reflectivity Z (indicated in plots by "ZCDNC"). This approach was implemented in SYRSOC and showed reasonable results.

2.2 The Data Set

The remote-sensing instruments mentioned above have been running automatically and continuously at Mace Head since 2009. For this part of the project, homogeneous single-layer non-precipitating water clouds were selected from the cloud radar data. Ceilometer data were available for 86% of the selected cloud cases detected by the radar and radiometer data for 81%. From the period from February 2009 to May 2015, 118 cloud cases were selected. Based on the 3-day back-trajectories from HYSPLIT (HYbrid Single-Particle Lagrangian Integrated Trajectory; Draxler and Rolph, 2014), the cloud cases were classified as marine, coming from the Atlantic ocean, or continental, coming from Europe. The classes “marine modified” and “continental modified” were introduced to classify ambiguous cases from the Atlantic but with brief transport paths over Ireland or Great Britain and cases from Europe with transport paths over the ocean, respectively. Of the 118 cases, 78 were classified as marine (60 marine and 18 marine modified) and 40 were classified as continental (26 continental and 14 continental modified). The selected cloud periods were each about 10–30 minutes long. With a temporal resolution of 10 seconds they provided over 18,000 time steps. In total, 8827 of the time steps were classified as marine, 2894 as marine modified, 4068 as continental and 2727 as continental modified.

2.3 Microphysical Cloud Properties

The results discussed in this section contain data for the entire cloud, except drizzle parts, which were excluded using a radar reflectivity threshold. The normalised distributions of the CDNC, effective radius and LWC are plotted in Figure 2.1 according to the air mass transport.

The medians and percentiles of the CDNC were smallest for marine and marine modified air masses. The distribution of marine cases was mono-modal, whereas the marine modified cases showed a bi-modal behaviour, with peaks at around 40 and 300 cm^{-3} . This indicates a mixture of air masses. It could also hint at misclassification of the air masses using back-trajectories in some ambiguous cases. Compared with the other air mass classes, rather few cloud cases were classified as marine modified or continental modified. This means that one outlier can contribute strongly to the distribution. The distribution

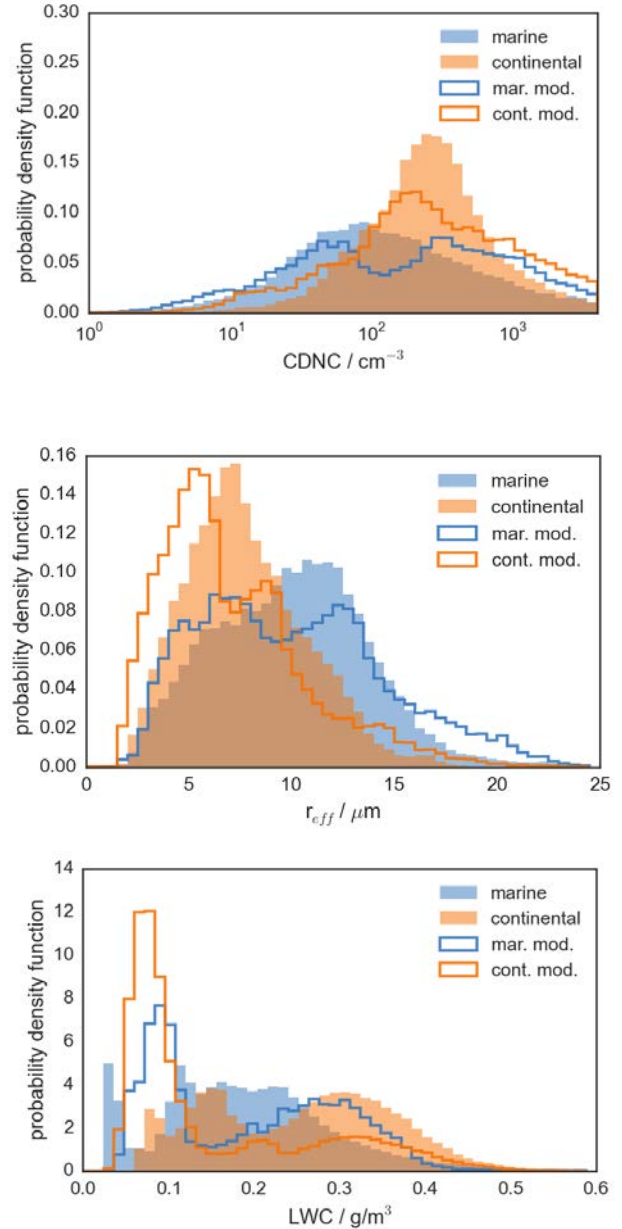


Figure 2.1. Distributions of CDNC (top, on logarithmic scale), effective radius (r_{eff} , centre) and LWC (bottom) by air mass transport. Modified air masses (mar. mod., marine modified; cont. mod., continental modified) are plotted as lines.

of the CDNC for the continental modified cases had one peak at around 160 cm^{-3} . However, the distribution stretched out to higher CDNCs, which can also be interpreted as an indicator for a mixture of air masses. The distribution for the continental cases had one distinct peak at around 250 cm^{-3} . On average, the CDNC was highest for continental cases, although small fractions of high CDNC were also found in all other air masses.

The distributions of the effective radius in marine and marine modified conditions were wider than in continental modified and continental conditions. In addition, the maximum frequencies were at higher effective radii. The median effective radius was $10\text{ }\mu\text{m}$ in marine and marine modified air masses. The distribution of the effective radius of marine modified cases was bi-modal, with one peak at around $7\text{ }\mu\text{m}$ and one at $14\text{ }\mu\text{m}$. Equivalent to the shape of the CDNC distribution, this indicates the influence of both clean and polluted air masses in this class. The continental modified cases also showed a bi-modal distribution for the same reasons mentioned before. One peak was at around $5\text{ }\mu\text{m}$ and one was at $9\text{ }\mu\text{m}$. The distribution of the effective radius in continental cases had one peak at $7\text{ }\mu\text{m}$.

These results confirm the inverse relationship between CDNC and effective radius, in agreement with the literature (Ferek *et al.*, 2000; Lohmann and Feichter, 2005). This relationship is forced by the algorithm at each time step. However, the data set studied here confirms the general validity of this assumption, using more than 18,000 time steps.

All distributions of CDNC and effective radius were broad, covering a wide range of values. This is because of the large number of data points and the coarse estimation of the air mass transport path 3 days prior to observation. The investigation of the actual origin of the air masses and the aerosol content at cloud level was not part of this study. Uncertainties in the classification would lead to broadening of the distributions. However, the shape and median of the distributions can be considered significant, because of the number of data points.

The distributions of the LWC showed two or more peaks for all classes. Whereas the 25th and 75th percentiles were similar for marine, marine modified and continental modified cases, the median of the continental modified cases was much lower because of a strong peak just below 0.1 g m^{-3} . The distributions in marine and marine modified conditions each had a smaller peak at 0.1 g m^{-3} , but also a second broader peak at around 0.2 g m^{-3} and 0.3 g m^{-3} , respectively. The distribution of the LWC of continental cases had several peaks as well, with the strongest at 1.5 g m^{-3} and 0.3 g m^{-3} . The median and 25th and 75th percentiles of the LWC distribution of continental air masses were highest. This seems contradictory;

however, drizzle was excluded from these data. The more polluted air masses advected from the continent could hold more liquid water before forming drizzle than the cleaner air masses from the ocean.

2.4 Optical Cloud Properties

The optical properties of all clouds were also investigated. Figure 2.2 shows the distributions of cloud optical thickness (COT) and the cloud albedo. The median and 25th and 75th percentiles of the COT were similar for marine, marine modified and continental modified cases (Preißler *et al.*, 2016). The main peaks of these distributions were at 1 and 3, 3 and 2, respectively. The two modified classes showed a slight second peak at a COT of around 6. The distribution of the continental cases looks very different. There is one sudden peak at a COT of 1 and a second very broad peak. The percentiles reflect this difference. The median, 25th and 75th percentiles were at 6, 3 and 11, respectively, the highest for this class.

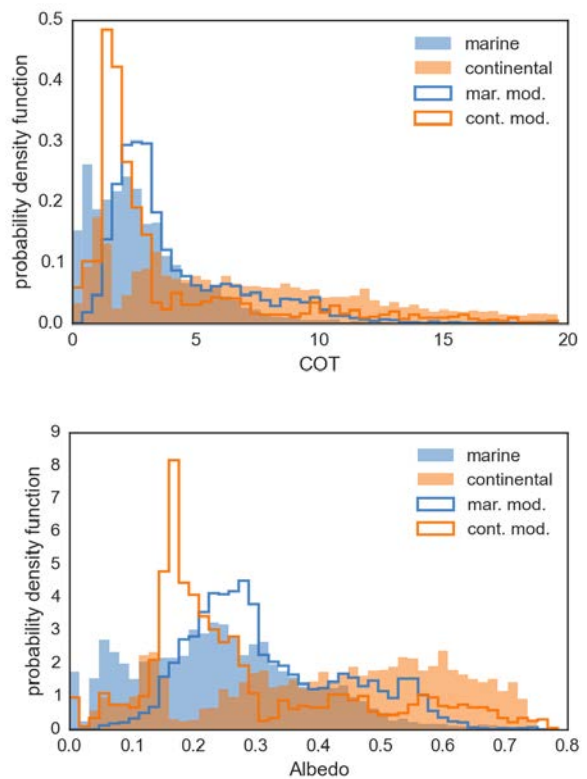


Figure 2.2. Distributions of COT (top) and cloud albedo (bottom) by air mass transport. Modified air masses (mar. mod., marine modified; cont. mod., continental modified) are plotted as lines.

Similar to the LWC, a very clear difference between the marine and modified classes and the continental class was found in the cloud albedo. Figure 2.2 shows two main peaks in the marine distribution at 0.05 and around 0.25, one broad peak in the marine modified distribution at 0.3 followed by a small peak at 0.45, one sharp peak in the continental modified distribution at 0.2, followed by some smaller peaks at much higher values (0.45 and 0.57), and a very broad distribution for continental cases, with mainly high albedos but a small peak at 0.12.

Overall, the COT and albedo were lower in cleaner air masses and higher in more polluted conditions, which is in agreement with the findings of Twomey (1977) and Brenguier *et al.* (2003) among others. In addition, the lower medians for the albedo and COT were linked to high medians for the effective radius and low medians for the CDNC (marine and marine modified cases) and vice versa (continental cases). The seemingly contradictory behaviour in continental modified cases can be attributed to a strong peak at low LWC. The minimum liquid water path (LWP) and, consequently, the lowest median subadiabaticity were found in continental modified cases (Preißler *et al.*, 2016). This did not impact the CDNC and effective radius, but strongly influenced the calculation of the COT and albedo.

2.5 Summary

Ground-based remote-sensing observations of cloud microphysical properties have been carried out at the coastal site of Mace Head since 2009. For this study, homogeneous single-layer non-precipitating water clouds were carefully selected from a database covering more than 6 years. This comprehensive study of 118 cloud cases with a total of more than 18,000 data points (time steps) can be considered to be statistically representative. The cloud properties were studied in terms of their dependence on the prevailing air mass at cloud level. The results presented in this chapter confirm the theory and previous findings of an increase in CDNC and decrease in effective radius with increasing pollution. It is important to validate such theories on a statistically significant scale, as achieved by using the large data set studied here. Generally, the median CDNC ranged from 60 cm^{-3} in marine air masses to 210 cm^{-3} in continental air masses. The median effective radius ranged from $6\text{ }\mu\text{m}$ in continental modified air to $10\text{ }\mu\text{m}$ in marine and marine modified air. The droplet size distributions were broader in marine cases and more distinct in continental cases. Overall, the COT and albedo were lower in cleaner air masses and higher in more polluted conditions, with medians ranging from 2 to 6 and 0.22 to 0.44, respectively. However, the calculation of the COT and albedo was strongly affected by the observed LWP and resulting subadiabaticity.

3 The Impact of Hemispheric Transboundary Air Pollution on Cloud Microphysics

The quantification of the impact of air pollution, transported towards Ireland from other countries in the Northern hemisphere, on cloud microphysics was another objective of this fellowship. This was partly addressed in the previous section. Additionally, transboundary air pollution was studied in greater detail and an attempt was made to quantify the transported aerosol mass. The aerosol detection described in the following section is running in near real-time, every 10 minutes. The results are displayed at <http://macehead.nuigalway.ie/rt/feature>.

3.1 Aerosol Detection

The ceilometer at Mace Head is used to detect aerosol layers and clouds up to about 15 km above ground level (agl). In the case of clouds, however, the detection limit depends on the COD. Furthermore, the detection efficiency of (weak) aerosol layers decreases with increasing altitude. Co-located with the ceilometer is a Doppler cloud radar, as mentioned previously. The radar signal is reflected by larger atmospheric particles such as cloud droplets, ice crystals, insects and very large aerosol particles; hence, the radar is not capable of detecting layers consisting of much smaller aerosol particles. Consequently, the classification of the different atmospheric features is based on the combination of data from the two instruments. From

the ceilometer, the background- and range-corrected backscatter signal is used for the feature analysis.

The radar data are used to supplement the ceilometer measurements with cloud information. Two examples of the so-called feature masks are shown in Figures 3.1 and 3.2. Figure 3.1 shows different cloud types, rain and the boundary layer aerosol, and some aerosol layers in the free troposphere observed on 20 May 2015.

To obtain the feature mask, all clouds are flagged using the cloud products provided by the radar (blue in Figures 3.1 and 3.2). The radar also provides information on the presence of rain, which is also flagged (orange in Figures 3.1 and 3.2). Periods when no aerosol retrieval is possible are flagged yellow. In the following steps, the remaining ceilometer data are classified according to the signal strength. This can be used as an indication for low/medium/high aerosol load (grey scale in Figures 3.1 and 3.2) and background noise. This is not suitable for an absolute quantitative evaluation. The particle backscatter and extinction coefficients or the aerosol mass can be obtained from ceilometer data only under certain assumptions (see the following section).

Volcanic eruptions in the past showed the importance of the observation and precise forecast of volcanic ash plumes for society and the economy. This is a crucial

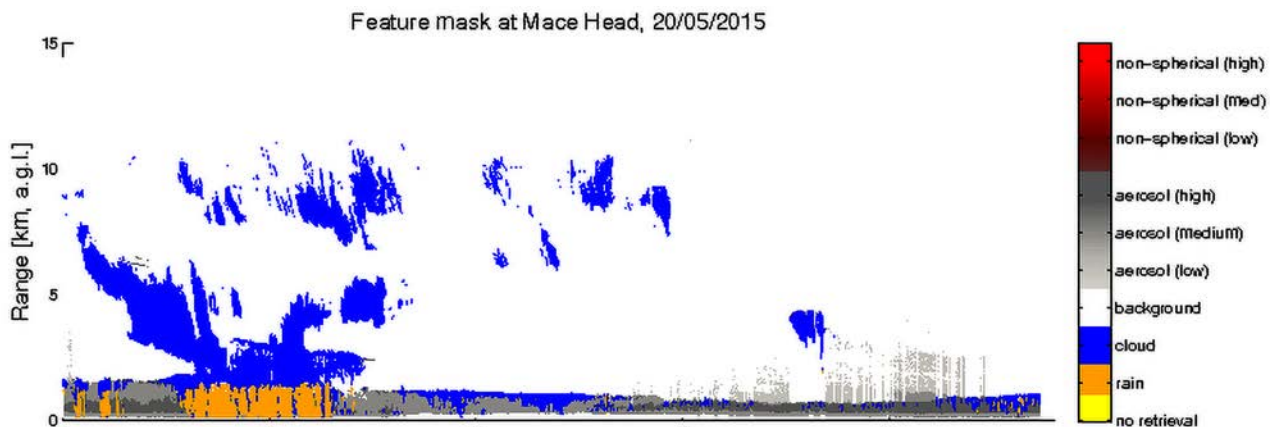


Figure 3.1. Aerosol detection product of observations from Mace Head on 20 May 2015. Time given in coordinated universal time (UTC). Local time on that day was UTC +1 hour.

application of transboundary air pollution detection. Volcanic ash particles are non-spherical and therefore depolarising. From ceilometer data alone it is not possible to distinguish non-spherical particles from spherical particles. The cloud radar data can help to make this distinction. However, as mentioned earlier, this is limited to large particles and is likely to miss free-tropospheric aerosol plumes. The radar-detected depolarisation ratio is used in the generation of the feature masks. Aerosol layers with sufficiently large non-spherical particles are classified as such (red scale in Figures 3.1 and 3.2).

Figure 3.2 shows the measurement from 19 April 2010, taken shortly after the eruption of Eyjafjallajökull in Iceland. The descending aerosol layers, presumably consisting of volcanic aerosol, are visible up to 4 km. When they become mixed into the boundary layer around noon, the depolarisation ratio detected by the radar indicates non-spherical particles, which are plotted in red.

This does not mean that all aerosol layers shown in grey consist of spherical particles only. Rather, it indicates that the other particles are too small to be detected by the radar. On the other hand, the presence of non-spherical particles does not necessarily indicate volcanic ash. Other non-spherical aerosol types with large scatterers can also be observed, for example desert dust.

3.2 Aerosol Quantification

Aerosols can be quantified in terms of particle extinction or backscatter coefficient and aerosol mass. For this part of the fellowship, data from a newly

installed Raman lidar were to be used. However, the instrument was faulty, as were two others intended for use at two other sites in Ireland. Consequently, the manufacturer Leosphere stopped support for its Raman lidars and recalled them, replacing them with Doppler wind lidars. These could not be used to obtain high-quality profiles of aerosol extinction and backscatter coefficients, however, as was expected from the Raman lidars. The back-up plan for this project was to use ceilometer backscatter data instead.

3.2.1 Ceilometer calibration

A so-called Rayleigh calibration (normalisation of the ceilometer attenuated backscatter with the molecular backscatter) was performed during clear nights; thus, the calibration constant was obtained. Theoretically, the assumption of a stable calibration constant for ceilometers is valid because the optical set-up does not change much in these simple systems. However, the calibration approach for the ceilometer backscatter coefficient, and consequently the extinction coefficient, is not valid for all cloud cases. The calibration constant cannot be used for daytime measurements, as the instrument changes the sensitivity of its detectors in order to protect them from overload due to high background radiation. The sensitivity is even further reduced in the case of low optically thick clouds because of the sudden peak in the received backscattered radiation. A daytime calibration of the ceilometer is possible by combination with sun photometer data. The integrated extinction profile of the ceilometer is matched to the aerosol optical depth determined by the sun photometer. The calibration constant thus obtained could be used for daytime

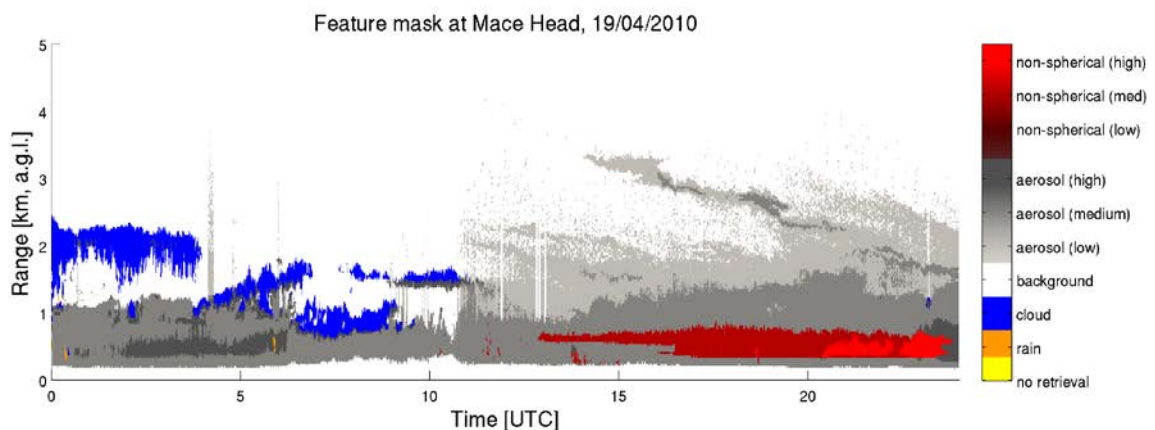


Figure 3.2. Aerosol detection product of observations from Mace Head on 19 April 2010. Time given in coordinated universal time (UTC).

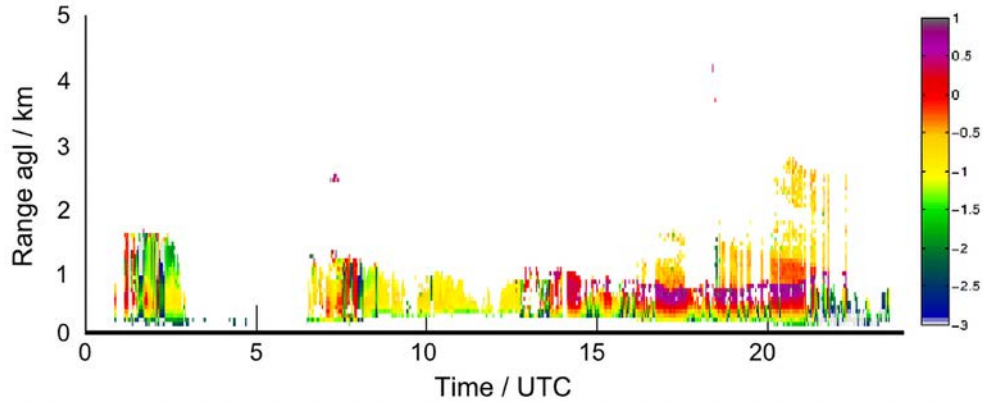


Figure 3.3. Logarithm of the extinction coefficient (in km^{-1}) from ceilometer observations on 20 May 2015.

measurements. However, this procedure could not be realised within the framework of this project.

3.2.2 Extinction estimation

For night-time periods without low clouds, the Rayleigh calibration can be applied to obtain particle backscatter coefficient profiles from ceilometer data. From these, the particle extinction coefficient can be calculated by assuming a constant extinction-to-backscatter ratio (or lidar ratio). The feature mask is used to limit the extinction retrieval to time periods and height regions with aerosol. Clouds, rain and background are excluded in order to save computational time. The procedure is illustrated below using data from 20 May 2015. The corresponding feature mask is shown in Figure 3.1.

The aerosol backscatter coefficient profiles are calculated using the so-called Klett algorithm. Assuming a fixed extinction-to-backscatter ratio (or lidar ratio) of 60 sr, the extinction coefficient profiles

are derived. Lidar ratios in this range were found for volcanic ash from Eyjafjallajökull at wavelengths of 355 and 532 nm using sophisticated multi-wavelength Raman lidars (Ansmann *et al.*, 2010). The aerosol extinction coefficient profiles for this example case are shown in Figure 3.3. Because of the problems with the calibration procedure, the daytime extinction coefficient is subject to large uncertainties. The effect of the change in sensitivity on the extinction data can be seen in Figure 3.3 at around 13:00 coordinated universal time (UTC), when the colour of the boundary layer changes rapidly and unrealistically from yellow to red (from about 0.1 km^{-1} to 1 km^{-1}).

3.2.3 Aerosol mass estimation

Profiles of the aerosol mass concentration were derived from the aerosol extinction coefficient using the mass-to-extinction ratio $\eta = \rho/\alpha$, with ρ being the mass concentration and α being the extinction. Hervo *et al.* (2012) found this ratio to be 1.57 g m^{-2} for

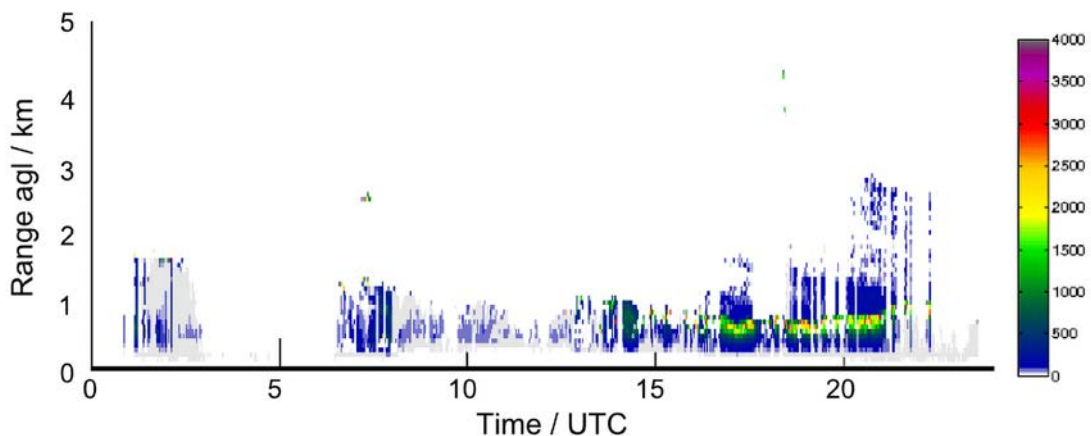


Figure 3.4. Aerosol mass concentration (in g m^{-2}) from ceilometer observations on 20 May 2015.

volcanic ash from Eyjafjallajökull and 0.33 g m^{-2} for local aerosol measured in central France. Therefore, in the near real-time retrieval η is set to 0.33 g m^{-2} when no volcanic ash alert has been issued. After a volcanic eruption with air mass advection towards Ireland, the value can be changed manually to 1.57 g m^{-2} . The value of the mass-to-extinction ratio used to produce the plot in Figure 3.4 was 0.33 g m^{-2} . As the mass is directly derived from the extinction profiles, the change in sensitivity of the ceilometer at around 13:00 UTC is also visible in the mass profiles.

3.3 Summary

A feature mask was developed by combining continuous ceilometer and cloud radar measurements

at Mace Head, Ireland. The product shows in near real-time the presence of boundary layer aerosol, clouds, rain and lofted aerosol layers at Mace Head. Plots are available online and are updated every 15 minutes (<http://macehead.nuigalway.ie/rt/feature.html>). The combination of the suite of remote-sensing instruments at Mace Head enables the detection of free tropospheric aerosol and a rough estimate of the quantitative properties of the aerosol plumes during night time. With the closest volcanic sources being located in Iceland, Mace Head is a prime site for the early detection of volcanic aerosol plumes. These remote-sensing data can be used to alert Ireland and Europe to volcanic aerosol advection in the case of westerly and north-westerly winds.

4 The Sensitivity of the Cloud Microphysical System to Both Natural and Anthropogenic Aerosols

This part of the project also required data from a sophisticated Raman lidar to accurately characterise the aerosol at cloud level. From Raman lidar observations, the lidar ratio can directly be derived. In combination with the ceilometer data, the Ångström exponent could also be obtained. Those two properties can be used to distinguish different aerosol types (Groß *et al.*, 2011; Burton *et al.*, 2012; Preißler *et al.*, 2013). Without the Raman lidar it was difficult to

separate natural from anthropogenic aerosols. Air mass transport was analysed for the cloud cases described in Chapter 2 using back-trajectories calculated at cloud level. A more detailed study determining the air mass origin (as opposed to the transport path) could be carried out, but the sensitivity study itself was not possible without the Raman lidar data.

5 WP 1: Retrieval of the Aerosol Optical Parameters

As described earlier, the new Raman lidar could not be used. The laser failed, which made operation of the system impossible. The quantification and characterisation of aerosol layers over Mace Head could therefore not be carried out in the proposed way. We used a different approach to estimate aerosol backscatter and extinction, which is, however, subject to larger uncertainties (see Chapter 3). Therefore, instead of a database of aerosol properties from lidar measurements, a database of cloud properties

from remote sensing and aerosol properties from ground-based *in situ* measurements was created. This database contains a large number of single-layer clouds, a subset of which was analysed for the work described in Chapter 2. For the same reason, the mass extinction coefficient could not be derived from lidar measurements. For an estimation of the mass load, we used values from the literature instead, as explained in section 3.2.3.

6 WP 2: Quantification of the Aerosol Indirect Effect

An attempt was made to quantify the AIE on microphysical cloud properties using remote-sensing observations in synergy with ground-based *in situ* aerosol measurements. A subset of cloud cases discussed in Chapter 2 was used for this study. Data from the AMS, SMPS, APS, ACSM and TEOM were available for 83%, 79%, 66%, 32% and 30% of the cloud cases, respectively. In order to verify the representativeness of the aerosol concentration levels near the surface with respect to aerosol concentration at cloud altitude, these observations were combined with the back-trajectory analysis described in Chapter 2. The following results (Figure 6.1) are also part of the recently submitted publication by Preißler *et al.* (2016).

In Figure 6.1 the distributions of black carbon (BC), CCN, sulfate (SO_4) and sea salt concentrations at ground level during the cloud observations are shown. The *in situ* data were not available for the

whole set of cloud cases. The number of data points in each distribution is shown on the top axis. Generally, concentrations of BC agreed well with the trajectory analysis, with higher concentrations for air masses advected from the continent and lower concentrations for air masses transported over the Atlantic. This is reflected in all mean values and percentiles shown, except the 95th percentile, which was higher for marine modified cases (240 ng m^{-3}) than for continental modified cases (220 ng m^{-3}). This was due to outliers with very high BC concentrations in marine modified air masses. The medians (and mean values) were 16 ng m^{-3} (23 ng m^{-3}) for marine cases, 18 ng m^{-3} (61 ng m^{-3}) for marine modified cases, 60 ng m^{-3} (78 ng m^{-3}) for continental modified cases and 127 ng m^{-3} (233 ng m^{-3}) for continental cases.

The lowest CCN mean value was found for marine modified cases, at 230 cm^{-3} ; the median value was

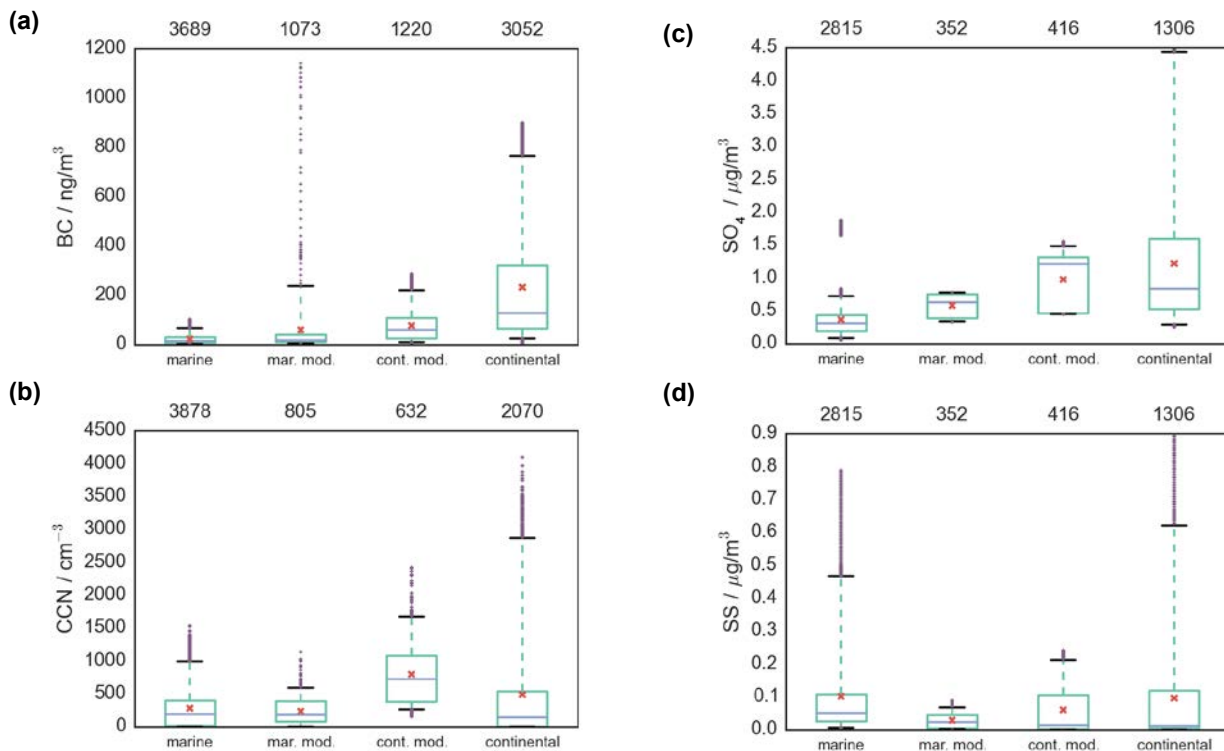


Figure 6.1. Box plots of the concentrations of (a) BC, (b) CCN, (c) SO_4 and (d) sea salt (SS), sorted by the air mass transport according to back-trajectories (mar. mod., marine modified; cont. mod., continental modified). Shown are the median (blue horizontal line), 25th and 75th percentiles (box), 5th and 95th percentiles (whiskers), mean (red cross) and data points outside the 5th–95th percentiles range (purple dots). The number of data points per class is shown on the top axis.

180 cm^{-3} . Both the median and the mean values for purely marine cases were similar to those for marine modified cases, at 190 cm^{-3} and 280 cm^{-3} , respectively. CCN concentrations of continental modified cases were, on average, highest, with median and mean values of 720 cm^{-3} and 790 cm^{-3} , respectively. The highest absolute values were observed during the presence of continental air masses. However, the median of this distribution was 140 cm^{-3} , which is similar to the means for the marine and marine modified cases. This indicates that there was no clear relationship between the CCN concentration and the air mass transport path. This result is because BC, SO_4 and sea salt can all act as CCN (Pierce and Adams, 2006; O'Dowd *et al.*, 1999).

The mean SO_4 concentration and the overall distribution represented the air masses well. During the majority of all marine cases, SO_4 concentrations below $0.7\text{ }\mu\text{g m}^{-3}$ were detected, with median and mean values of $0.31\text{ }\mu\text{g m}^{-3}$ and $0.37\text{ }\mu\text{g m}^{-3}$, respectively. All percentiles were higher for marine modified cases and, again, for continental modified cases. The median (and mean) values for these two classes were $0.63\text{ }\mu\text{g m}^{-3}$

($0.58\text{ }\mu\text{g m}^{-3}$) and $1.21\text{ }\mu\text{g m}^{-3}$ ($0.97\text{ }\mu\text{g m}^{-3}$), respectively. The highest SO_4 concentrations were observed during the presence of continental air masses.

The sea salt concentrations are not indicative of the air mass transport to Mace Head. At such a coastal site, sea salt is generally present and concentrations depend more on the wind speed at the time of observation and along the trajectory than on the advection path. The overall spread of the sea salt concentrations reflects the number of data points, with larger spreads for the marine and continental classes with high numbers of data points and less spread for the two modified classes with fewer data points. The median (and mean) values were $0.05\text{ }\mu\text{g m}^{-3}$ ($0.10\text{ }\mu\text{g m}^{-3}$) for marine cases, $0.02\text{ }\mu\text{g m}^{-3}$ ($0.03\text{ }\mu\text{g m}^{-3}$) for marine modified cases, $0.01\text{ }\mu\text{g m}^{-3}$ ($0.06\text{ }\mu\text{g m}^{-3}$) for continental modified cases and $0.01\text{ }\mu\text{g m}^{-3}$ ($0.10\text{ }\mu\text{g m}^{-3}$) for continental cases.

The plots in Figures 6.2–6.4 show frequency distributions of the cloud droplet effective radius, CDNC, LWC and COD, depending on the concentration of condensation nuclei from the CCN

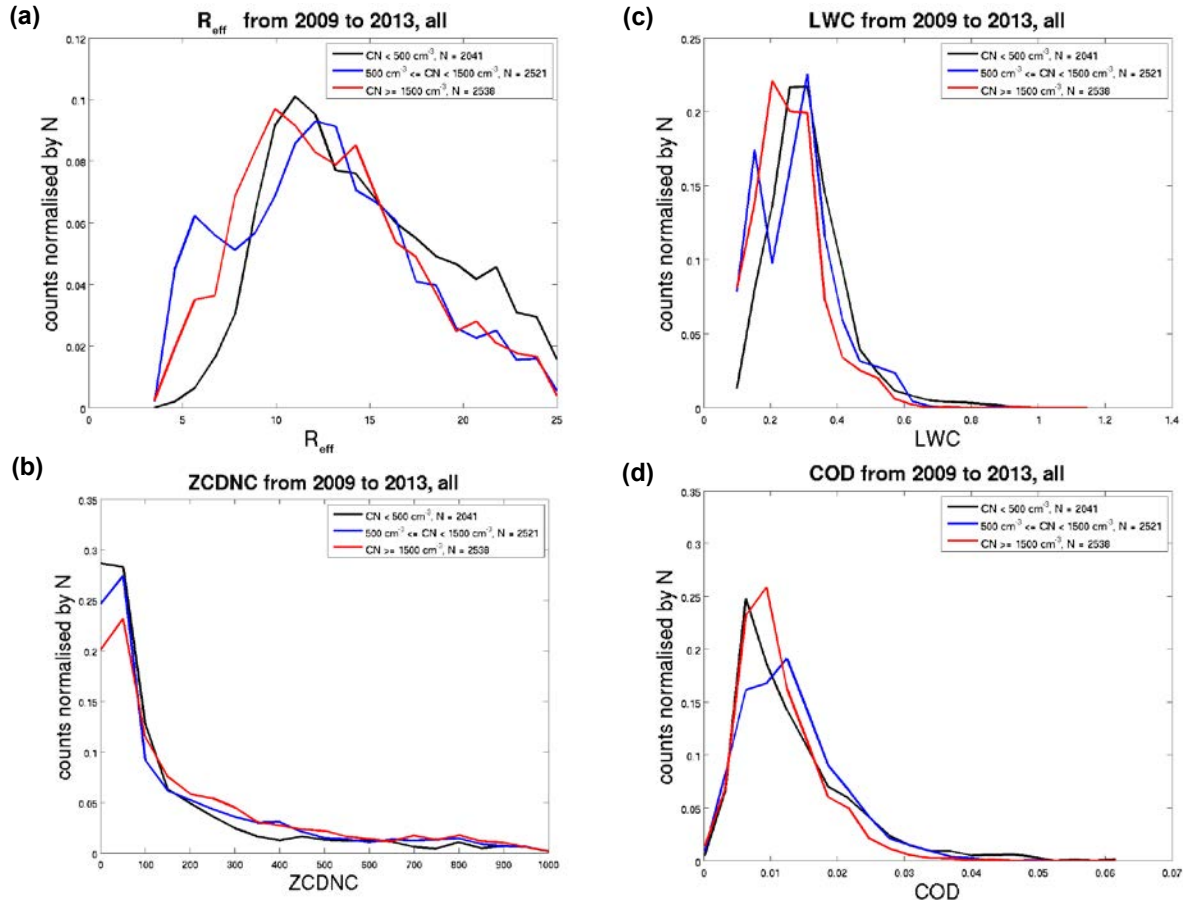


Figure 6.2. Distributions of (a) the effective radius, (b) CDNC, (c) LWC and (d) COD by condensation nuclei (CN) concentration.

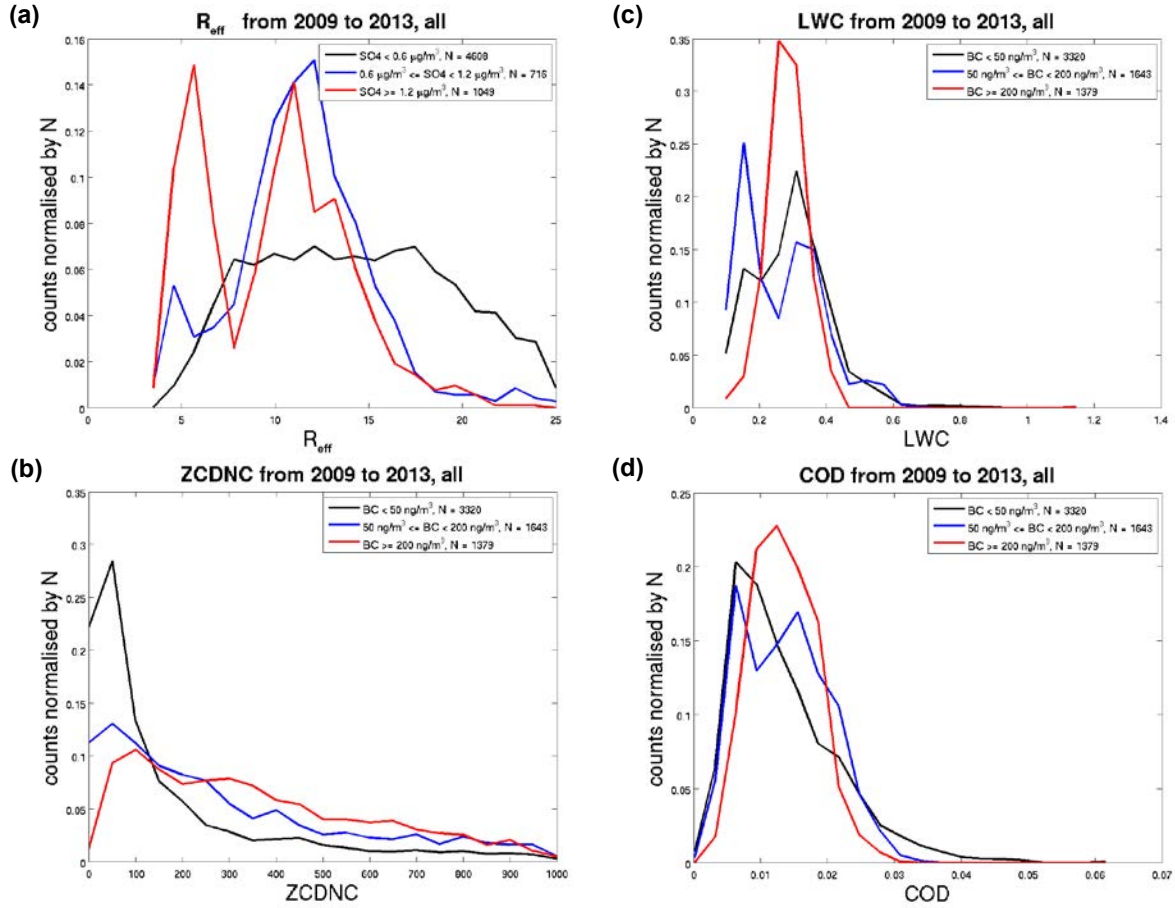


Figure 6.3. Distributions of (a) the effective radius, (b) CDNC, (c) LWC and (d) COD by BC concentration.

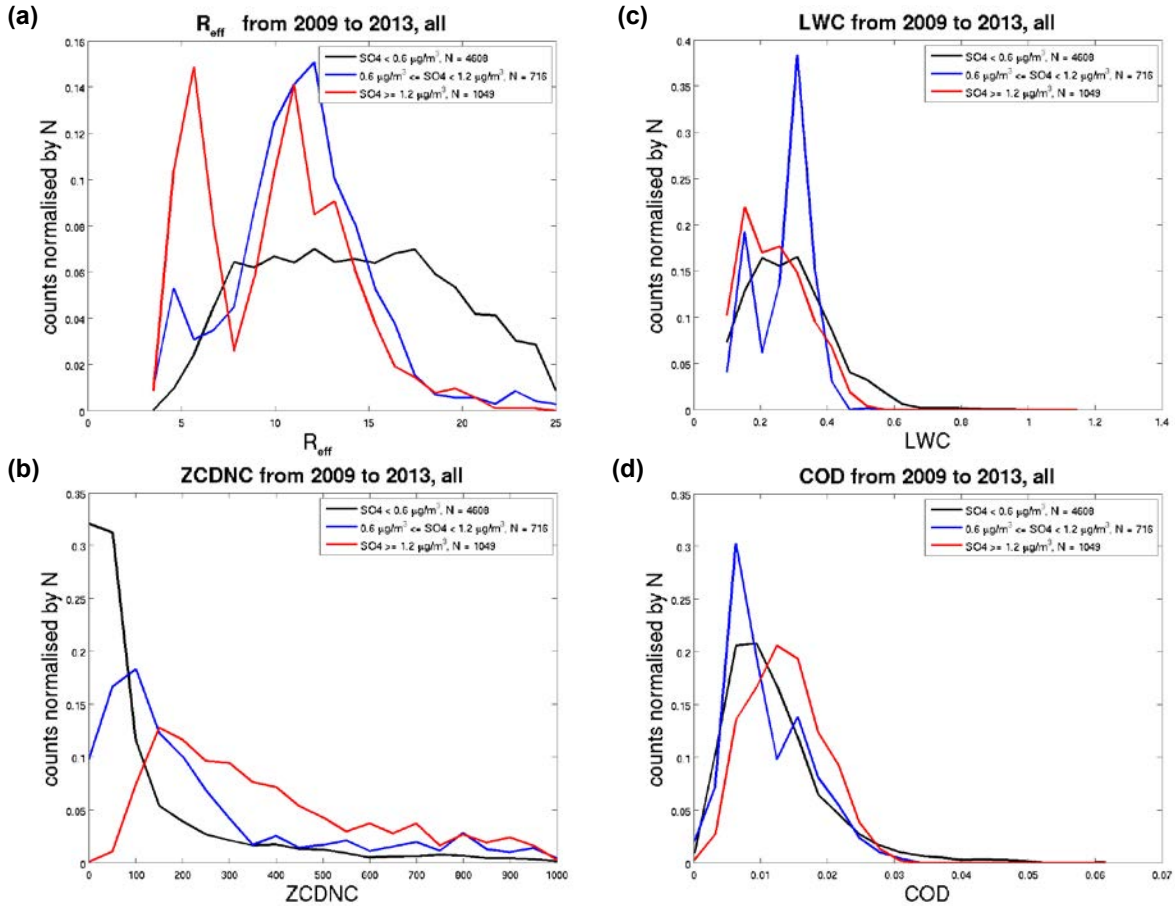


Figure 6.4. Distributions of (a) the effective radius, (b) CDNC, (c) LWC and (d) COD by SO_4 concentration.

counter (Figure 6.2), BC measured by the multi-angle absorption photometer (Figure 6.3) and SO_4 from AMS measurements (Figure 6.4).

The cloud properties did not depend strongly on the condensation nuclei concentration. On average, the effective radius was slightly higher at lower condensation nuclei concentrations. The CDNC derived from the radar reflectivity Z (indicated in plots by “ZCDNC”), the LWC and the COD did not show clear differences.

The BC concentration had a stronger impact on the cloud properties. Clear differences in the distributions of the effective radius and CDNC are shown in Figure 6.3. The effective radii were larger at low BC concentrations and smaller at medium and high BC concentrations. The CDNC shows the opposite behaviour, with a large CDNC at high BC concentrations and a rather low CDNC at low BC concentrations. The average COD is slightly higher at high BC concentrations. The LWC did not show a dependency on BC concentrations.

The impact of SO_4 concentrations on the microphysical cloud properties was similar to the effect of BC, as shown in Figure 6.4. The effective radii were largest at low SO_4 concentrations and smallest at high SO_4 concentrations. In addition, the CDNC was highest at high SO_4 concentrations and rather low at low SO_4 concentrations. The average COD was slightly higher at high SO_4 concentrations.

The LWC did not show a dependency on any of the studied pollutants. This finding is consistent with the observation of the inverse relationship between the effective radius and the CDNC, which is valid only in the case of constant LWC.

The AIE was investigated for different aerosol and cloud proxies, following the approach of Feingold *et al.* (2001). They proposed the following index:

$$\text{AIE} = -\delta \log(C_{\text{var}}) / \delta \log(A_{\text{var}}) \quad (6.1)$$

where C_{var} is the cloud proxy and A_{var} is the aerosol proxy. Feingold *et al.* (2001) used the cloud droplet effective radius as a cloud proxy and the particle

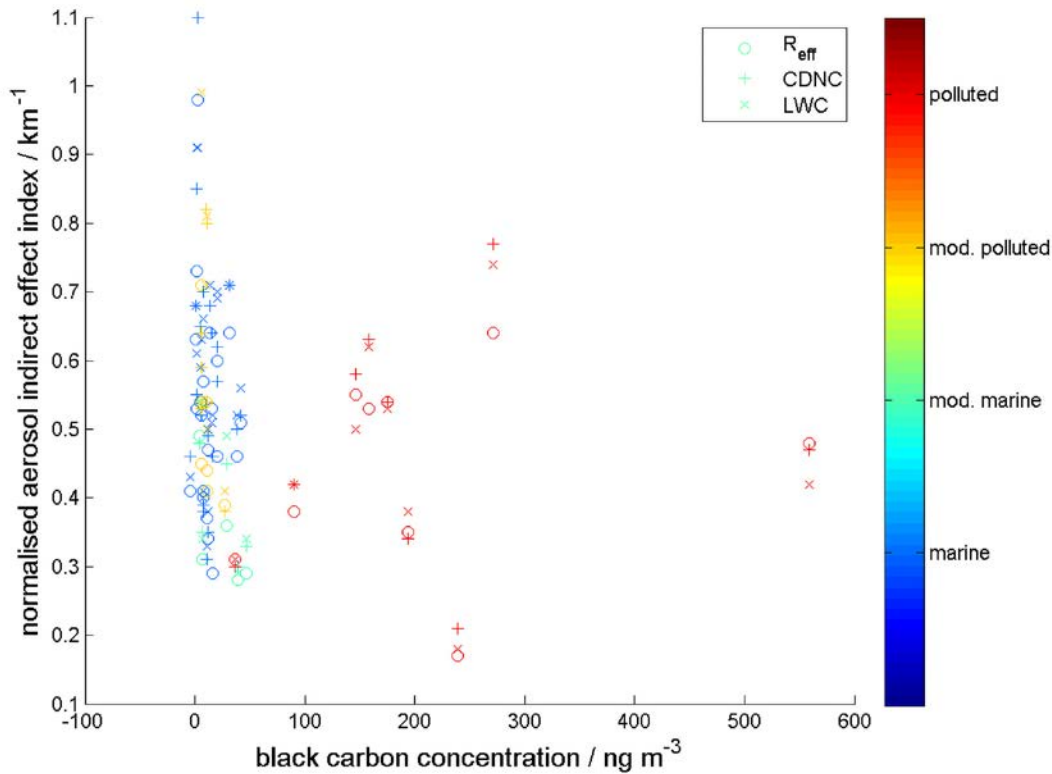


Figure 6.5. Aerosol indirect effect normalised by cloud depth using different cloud proxies (symbols) vs. the BC concentration, colour coded by air mass transport path. R_{eff} , effective radius.

extinction coefficient as an aerosol proxy. In the framework of this fellowship, different aerosol and cloud proxies were tested for applicability. However, the uncertainties in the aerosol proxies from ceilometer measurements alone are too large to draw robust conclusions. For this part of the study, again a subset of cloud cases described in Chapter 2 was used.

In Figure 6.5 the AIE for different cloud parameters versus the BC concentration are shown, colour coded by the air mass transport. The aerosol proxy was the extinction estimate from the ceilometer measurements described in section 3.2.2. As cloud proxies, the effective radius, CDNC and LWC were tested.

The range of values was very large and no relationship between the normalised AIE and the BC concentration or the AIE and the air mass transport was found. This finding was tested for other aerosol components such as SO_4 , organics, sea salt and nitrate (NO_3), with similar results. Case by case, the three cloud proxies seem to behave similarly, which is clearly visible in Figure 6.5 for the cases with high BC concentrations, as all three symbols are clustered around similar values of normalised AIE.

7 Summary and Conclusions

We used a synergistic combination of long-term *in situ* and remote-sensing observations in an attempt to reduce the uncertainty in the impact of both natural marine and anthropogenic aerosols on clouds and cloud optical properties. Homogeneous single-layer non-precipitating water clouds were carefully selected from a database covering more than 6 years. This comprehensive study of 118 cloud cases with a total of more than 18,000 data points (time steps) can be considered to be statistically representative. The dependence of the cloud properties on the prevailing air mass at cloud level was studied. The results confirm the theory and previous findings of an increase in CDNC and decrease in cloud droplet effective radius with increasing pollution. The median CDNC ranged from 60 cm^{-3} in marine air masses to 210 cm^{-3} in continental air masses. The median effective radius ranged from $6\text{ }\mu\text{m}$ in continental modified air to $10\text{ }\mu\text{m}$ in marine and marine modified air. Overall, the COT and albedo were lower in cleaner air masses and higher in more polluted conditions, with median values ranging from 2 to 6 and 0.22 to 0.44, respectively.

The combination of the suite of remote-sensing instruments at Mace Head enables the detection

of free tropospheric aerosol layers. However, the quantification of aerosols in terms of particle extinction coefficients and mass concentrations could not be realised as originally proposed because of problems with the newly purchased Raman lidar. The Raman lidar could not be used because of a failure of the laser. Ceilometer data were used instead to quantify aerosols within limitations and under large uncertainties. Mace Head is a prime site for the early detection of volcanic aerosol plumes and other trans-boundary air pollution. The aerosol detection results are available online and can be used to alert Ireland and Europe of aerosol advection in the case of westerly and north-westerly winds.

To quantify the AIE on microphysical cloud properties using remote-sensing observations in synergy with ground-based *in situ* aerosol measurements, data from the AMS, SMPS, APS, ACSR and TEOM were used instead of the initially proposed Raman lidar data. In order to verify the representativeness of the aerosol concentration levels near the surface with respect to aerosol concentration at cloud altitude, these observations were combined with the analysis of 3-day back-trajectories.

8 Recommendations

- Development and implementation of a more sophisticated calibration procedure for the ceilometer for improved aerosol quantification.
- Investigation of aerosol origin (and thus type) by calculating longer back-trajectories and combining them with aerosol transport models.
- Characterisation of the impact of these different aerosol types on cloud properties.
- Adding more cases to the database of cloud and aerosol properties.
- Comparison of the results of different drizzle screening approaches and application of the most robust approach or a combination of approaches.
- In-depth comparison of SYRSOC results with the results from other algorithms, model data and satellite data.
- Implementation of automatic runs of SYRSOC for a near real-time calculation of microphysical cloud properties.
- Use of network data from EARLINET (European Aerosol Research Lidar Network; www.earlinet.org) or E-Profile (www.eumetnet.eu/alc-network) and satellite data for detailed analysis of trans-boundary air pollution.

References

- Ansmann, A., Tesche, M., Gross, S., Freudenthaler, V., Seifert, P., Hiebsch, A., Schmidt, J., Wandinger, U., Mattis, I., Mueller, D. and Wiegner, M., 2010. The 16 April 2010 major volcanic ash plume over central Europe: EARLINET lidar and AERONET photometer observations at Leipzig and Munich, Germany. *Geophysical Research Letters* 37: L13810.
- Bauer-Pfundstein, M.R. and Goersdorf, U., 2007. Target separation and classification using cloud radar Doppler-spectra. *Proceedings of the 33rd Conference on Radar Meteorology*. Available online: https://ams.confex.com/ams/33Radar/techprogram/paper_123456.htm (accessed 28 November 2018).
- Brenguier, J.-L., Pawlowska, H. and Schüller, L., 2003. Cloud microphysical and radiative properties for parameterization and satellite monitoring of the indirect effect of aerosol on climate. *Journal of Geophysical Research* 108: 8632.
- Burton, S.P., Ferrare, R.A., Hostetler, C.A., Hair, J.W., Rogers, R.R., Obland, M.D., Butler, C.F., Cook, A.L., Harper, D.B. and Froyd, K.D., 2012. Aerosol classification using airborne high spectral resolution lidar measurements methodology and examples. *Atmospheric Measurement Techniques* 5: 73–98.
- Crewell, S. and Löhnert, U., 2003. Accuracy of cloud liquid water path from ground-based microwave radiometry 2. Sensor accuracy and synergy. *Radio Science* 38: 8042.
- Draxler, R.R. and Rolph, G.D., 2014. HYSPLIT (HYbrid Single-Particle Lagrangian Integrated Trajectory) Model. NOAA Air Resources Laboratory, Silver Spring, MD, USA. Available online: <http://ready.arl.noaa.gov/HYSPLIT.php> (accessed 23 November 2018).
- Feingold, G., Remer, L.A., Ramaprasad, J. and Kaufman, Y.J., 2001. Analysis of smoke impact on clouds in Brazilian biomass burning regions: an extension of Twomey's approach. *Journal of Geophysical Research* 106: 22907–22922.
- Ferek, R.J., Garrett, T., Hobbs, P.V., Strader, S., Johnson, D., Taylor, J.P., Nielsen, K., Ackerman, A.S., Kogan, Y., Liu, Q., Albrecht, B.A. and Babb, D., 2000. Drizzle suppression in ship tracks. *Journal of the Atmospheric Sciences* 57: 2707–2728.
- Groß, S., Tesche, M., Freudenthaler, V., Toledano, C., Wiegner, M., Ansmann, A., Althausen, D. and Seefeldner, M., 2011. Characterization of Saharan dust, marine aerosols and mixtures of biomass-burning aerosols and dust by means of multi-wavelength depolarization and Raman lidar measurements during SAMUM 2. *Tellus* 63B: 706–724.
- Heese, B., Flentje, H., Althausen, D., Ansmann, A. and Frey, S., 2010. Ceilometer lidar comparison: backscatter coefficient retrieval and signal-to-noise ratio determination. *Atmospheric Measurement Techniques* 3: 1763–1770.
- Hervo, M., Quennehen, B., Kristiansen, N.I., Boulon, J., Stohl, A., Fréville, P., Pichon, J.-M., Picard, D., Labazuy, P., Gouhier, M., Roger, J.-C., Colomb, A., Schwarzenboeck, A. and Sellegri, K., 2012. Physical and optical properties of 2010 Eyjafjallajökull volcanic eruption aerosol: ground-based, lidar and airborne measurements in France. *Atmospheric Chemistry and Physics* 12: 1721–1736.
- Lohmann, U. and Feichter, J., 2005. Global indirect aerosol effects: a review. *Atmospheric Chemistry and Physics* 5: 715–737.
- Löhnert, U. and Crewell, S., 2003. Accuracy of cloud liquid water path from ground-based microwave radiometry 1. Dependency on cloud model statistics. *Radio Science* 38: 8041.
- Löhnert, U., Turner, D.D. and Crewell, S., 2009. Ground-based temperature and humidity profiling using spectral infrared and microwave observations. Part I: simulated retrieval performance in clear-sky conditions. *Journal of Applied Meteorology and Climatology* 48: 1017–1032.
- Martucci, G. and O'Dowd, C.D., 2011. Ground-based retrieval of continental and marine warm cloud microphysics. *Atmospheric Measurement Techniques* 4: 2749–2765.
- Martucci, G., Milroy, C. and O'Dowd, C.D., 2010. Detection of cloud base using Jenoptik CHM15K and Vaisala CL31 ceilometers. *Journal of Atmospheric and Oceanic Technology* 27: 305–318.
- Melchionna, S., Bauer, M. and Peters, G., 2008. A new algorithm for the extraction of cloud parameters using multipeak analysis of cloud radar data. First application and results. *Meteorologische Zeitschrift* 17: 613–620.

- O'Dowd, C.D., Lowe, J.A. and Smith, M.H., 1999. Coupling sea-salt and sulphate interactions and its impact on cloud droplet concentration predictions. *Geophysical Research Letters* 26: 1311–1314.
- Pierce, J.R. and Adams, P.J., 2006. Global evaluation of CCN formation by direct emission of sea salt and growth of ultrafine sea salt. *Journal of Geophysical Research* 111: D06203.
- Preißler, J., Wagner, F., Guerrero-Rascado, J.L. and Silva, A.M., 2013. A two-year climatology of free-tropospheric aerosol layers over Portugal observed by lidar. *Journal of Geophysical Research: Atmospheres* 118: 3676–3686.
- Preißler, J., Martucci, G., Saponaro, G., Kolmonen, P., Sogacheva, L., de Leeuw, G. and O'Dowd, C., 2016. Six years ground-based remote sensing of microphysical properties of stratiform liquid clouds at Mace Head, Ireland. *Journal of Geophysical Research: Atmospheres* 121: 14538–14557.
- Solomon, S., Qin, D., Manning, M., Chen, Z., Marquis, M., Averyt, K.B., Tigno, M. and Miller, H.L. (eds), 2007. *Climate Change 2007: The Physical Science Basis*. Contribution of Working Group I to the Fourth Assessment Report of the Intergovernmental Panel on Climate Change. Cambridge University Press, Cambridge.
- Stocker, T.F., Qin, D., Plattner, G.-K., Tignor, M., Allen, S.K., Boschung, J., Nauels, A., Xia, Y., Bex, V. and Midgley, P.M. (eds), 2013. *Climate Change 2013: The Physical Science Basis*. Contribution of Working Group I to the Fifth Assessment Report of the Intergovernmental Panel on Climate Change. Cambridge University Press, Cambridge.
- Twomey, S., 1977. The influence of pollution on shortwave albedo of clouds. *Journal of the Atmospheric Sciences* 34: 1149–1152.

Abbreviations

ACSM	Aerosol chemical speciation monitor
agl	Above ground level
AIE	Aerosol indirect effect
AMS	Aerosol mass spectrometer
APS	Aerodynamic particle sizer
BC	Black carbon
CCN	Cloud condensation nuclei
CDNC	Cloud droplet number concentration
COD	Cloud optical depth
COT	Cloud optical thickness
HR-TOF	High-resolution time of flight
LWC	Liquid water content
LWP	Liquid water path
SMPS	Scanning mobility particle sizer
SO ₄	Sulfate
SYRSOC	SYnergistic Remote Sensing Of Clouds
TEOM	Tapered element oscillating microbalance
UTC	Coordinated universal time

AN GHNÍOMHAIREACHT UM CHAOMHNÚ COMHSHAOIL
Tá an Gníomhaireacht um Chaomhnú Comhshaoil (GCC) freagrach as an gcomhshaol a chaomhnú agus a fheabhsú mar shócmhainn luachmhar do mhuintir na hÉireann. Táimid tiomanta do dhaoine agus don chomhshaol a chosaint ó éifeachtaí díobhálacha na radaíochta agus an truaillithe.

Is féidir obair na Gníomhaireachta a roinnt ina trí phríomhréimse:

Rialú: Déanaimid córais éifeachtacha rialaithe agus comhlionta comhshaoil a chur i bhfeidhm chun torthaí maithe comhshaoil a sholáthar agus chun díriú orthu siúd nach gcloíonn leis na córais sin.

Eolas: Soláthraimid sonraí, faisnéis agus measúnú comhshaoil atá ar ardchaighdeán, spriocdhírthe agus tráthúil chun bonn eolais a chur faoin gcinnteoireacht ar gach leibhéal.

Tacaíocht: Bimid ag saothrú i gcomhar le grúpaí eile chun tacú le comhshaol atá glan, táirgiúil agus cosanta go maith, agus le hiompar a chuirfidh le comhshaol inbhuanaithe.

Ár bhFreagrachtaí

Ceadúnú

Déanaimid na gníomhaíochtaí seo a leanas a rialú ionas nach ndéanann siad dochar do shláinte an phobail ná don chomhshaol:

- saoráidí dramhaíola (*m.sh. láithreáin líonta talún, loisceoirí, stáisiúin aistrithe dramhaíola*);
- gníomhaíochtaí tionsclaíocha ar scála mór (*m.sh. déantúsaíocht cógaisíochta, déantúsaíocht stroighne, stáisiúin chumhachta*);
- an diantalmhaíocht (*m.sh. muca, éanlaith*);
- úsáid shrianta agus scaoileadh rialaithe Orgánach Géinmhodhnaithe (*OGM*);
- foinsí radaíochta ianúcháin (*m.sh. trealamh x-gha agus radaiteiripe, foinsí tionsclaíocha*);
- áiseanna móra stórála peitril;
- scardadh dramhuisce;
- gníomhaíochtaí dumpála ar farraige.

Forfheidhmiú Náisiúnta i leith Cúrsaí Comhshaoil

- Clár náisiúnta iniúchtaí agus cigireachtaí a dhéanamh gach bliain ar shaoráidí a bhfuil ceadúnas ón nGníomhaireacht acu.
- Maoirseacht a dhéanamh ar fhreagrachtaí cosanta comhshaoil na n-údarás áitiúil.
- Caighdeán an uisce óil, arna sholáthar ag soláthraithe uisce phoiblí, a mhaoirsiú.
- Obair le húdaráis áitiúla agus le gníomhaireachtaí eile chun dul i ngleic le coireanna comhshaoil trí chomhordú a dhéanamh ar líonra forfheidhmiúcháin náisiúnta, trí dhíriú ar chiontóirí, agus trí mhaoirsiú a dhéanamh ar leasúchán.
- Cur i bhfeidhm rialachán ar nós na Rialachán um Dhramhthrealamh Leictreach agus Leictreonach (DTLL), um Shrian ar Shubstaintí Guaiseacha agus na Rialachán um rialú ar shubstaintí a ídionn an ciseal ózóin.
- An dlí a chur orthu siúd a bhriseann dlí an chomhshaoil agus a dhéanann dochar don chomhshaol.

Bainistíocht Uisce

- Monatóireacht agus tuairisciú a dhéanamh ar cháilíocht aibhneacha, lochanna, uisce idirchriosacha agus cósta na hÉireann, agus screamhuisc; leibhéil uisce agus sruthanna aibhneacha a thomhas.
- Comhordú náisiúnta agus maoirsiú a dhéanamh ar an gCreat-Treoir Uisce.
- Monatóireacht agus tuairisciú a dhéanamh ar Cháilíocht an Uisce Snámha.

Monatóireacht, Anailís agus Tuairisciú ar an gComhshaol

- Monatóireacht a dhéanamh ar cháilíocht an aeir agus Treoir an AE maidir le hAer Glan don Eoraip (CAFÉ) a chur chun feidhme.
- Tuairisciú neamhspleách le cabhrú le cinnteoireacht an rialtais náisiúnta agus na n-údarás áitiúil (*m.sh. tuairisciú tréimhsiúil ar staid Chomhshaol na hÉireann agus Tuarascálacha ar Tháscairí*).

Rialú Astaíochtaí na nGás Ceaptha Teasa in Éirinn

- Fardail agus réamh-mheastacháin na hÉireann maidir le gáis cheaptha teasa a ullmhú.
- An Treoir maidir le Trádáil Astaíochtaí a chur chun feidhme i gcomhair breis agus 100 de na táirgeoirí dé-ocsaíde carbóin is mó in Éirinn.

Taighde agus Forbairt Comhshaoil

- Taighde comhshaoil a chistiú chun brúnna a shainaitheint, bonn eolais a chur faoi bheartais, agus réitigh a sholáthar i réimsí na haeráide, an uisce agus na hinbhuanaitheachta.

Measúnacht Straitéiseach Timpeallachta

- Measúnacht a dhéanamh ar thionchar pleananna agus clár beartaithe ar an gcomhshaol in Éirinn (*m.sh. mórfhleananna forbartha*).

Cosaint Raideolaíoch

- Monatóireacht a dhéanamh ar leibhéil radaíochta, measúnacht a dhéanamh ar nochtadh mhuintir na hÉireann don radaíocht ianúcháin.
- Cabhrú le pleananna náisiúnta a fhorbairt le haghaidh éigeandálaí ag eascairt as taismí núicléacha.
- Monatóireacht a dhéanamh ar fhorbairtí thar lear a bhaineann le saoráidí núicléacha agus leis an tsábháilteacht raideolaíochta.
- Sainseirbhísí cosanta ar an radaíocht a sholáthar, nó maoirsiú a dhéanamh ar sholáthar na seirbhísí sin.

Treoir, Faisnéis Inrochtana agus Oideachas

- Comhairle agus treoir a chur ar fáil d’earnáil na tionsclaíochta agus don phobal maidir le hábhair a bhaineann le caomhnú an chomhshaoil agus leis an gcosaint raideolaíoch.
- Faisnéis thráthúil ar an gcomhshaol ar a bhfuil fáil éasca a chur ar fáil chun rannpháirtíocht an phobail a spreagadh sa chinnteoireacht i ndáil leis an gcomhshaol (*m.sh. Timpeall an Tí, léarscáileanna radóin*).
- Comhairle a chur ar fáil don Rialtas maidir le hábhair a bhaineann leis an tsábháilteacht raideolaíoch agus le cúrsaí práinnfhreagartha.
- Plean Náisiúnta Bainistíochta Dramhaíola Guaisí a fhorbairt chun dramhaíl ghuaiseach a chosaint agus a bhainistiú.

Múscailt Feasachta agus Athrú Iompraíochta

- Feasacht chomhshaoil níos fearr a ghiniúint agus dul i bhfeidhm ar athrú iompraíochta dearfach trí thacú le gnóthais, le pobail agus le teaghlaigh a bheith níos éifeachtúla ar acmhainní.
- Tástáil le haghaidh radóin a chur chun cinn i dtithe agus in ionaid oibre, agus gníomhartha leasúcháin a spreagadh nuair is gá.

Bainistíocht agus struchtúr na Gníomhaireachta um Chaomhnú Comhshaoil

Tá an ghníomhaíocht á bainistiú ag Bord lánaimseartha, ar a bhfuil Ard-Stiúrthóir agus cúigear Stiúrthóirí. Déantar an obair ar fud cúig cinn d’Oifigí:

- An Oifig um Inmharthanacht Comhshaoil
- An Oifig Forfheidhmithe i leith cúrsaí Comhshaoil
- An Oifig um Fianaise is Measúnú
- Oifig um Chosaint Radaíochta agus Monatóireachta Comhshaoil
- An Oifig Cumarsáide agus Seirbhísí Corparáideacha

Tá Coiste Comhairleach ag an nGníomhaireacht le cabhrú léi. Tá dáréag comhaltaí air agus tagann siad le chéile go rialta le plé a dhéanamh ar ábhair inní agus le comhairle a chur ar an mBord.

Authors: Jana Preißler, Giovanni Martucci
and Colin D. O'Dowd

Clouds and aerosols play an important part in climate processes; however, their interactions are not well understood. To study the effect of both natural marine and anthropogenic aerosols on clouds and cloud optical properties we looked at a mix of information from remote-sensing and in situ instruments from more than 6 years. This mix of information helped to obtain the aerosol load near the surface and at cloud base, as well as cloud properties. Our findings support both theory and earlier findings of more, but smaller, cloud droplets when the aerosol load is larger. Clouds appear brighter in more polluted conditions, reflecting more sunlight back into space.

Identifying Pressures

Environmental pressures that this fellowship identified are related to the anthropogenic impact on air quality, weather and climate. The interaction of man-made and naturally occurring pollutants with clouds, and thus their impact on the climate, were studied with the help of remote-sensing instruments.

Informing Policy

Research findings have been published in peer-reviewed journals and presented at international workshops and conferences. In addition, regular reports have been provided to inform policymakers. The following topics were addressed: cloud and aerosol properties, their interaction and their impact on climate.

Developing Solutions

This fellowship enabled maintenance of the remote-sensing division at Mace Head Atmospheric Research Station on the west coast of Ireland. Sophisticated sensors on the ground enabled highly temporally and vertically resolved observations of atmospheric components. An advancement of methodologies as well as use of a large data set led to an improved understanding of aerosol–cloud interactions, which was communicated to both the scientific and the non-scientific communities.